

# Measurement of the magneto-optical response of Fe and CrO<sub>2</sub> epitaxial films by pump-probe spectroscopy: Evidence for spin-charge separation

E. Carpene\*

*IFN-CNR, Dipartimento di Fisica, Politecnico di Milano, 20133 Milan, Italy*

F. Boschini, H. Hedayat, C. Piovera, and C. Dallera

*Dipartimento di Fisica, Politecnico di Milano, 20133 Milan, Italy*

E. Puppin

*CNISM, Dipartimento di Fisica, Politecnico di Milano, 20133 Milan, Italy*

M. Mansurova and M. Münzenberg

*I. Physikalisches Institut, Georg-August-Universität Göttingen, 37077 Göttingen, Germany*

X. Zhang and A. Gupta

*Department of Chemistry, University of Alabama, Tuscaloosa, Alabama 35487, USA*

(Received 28 February 2013; revised manuscript received 29 April 2013; published 31 May 2013)

We have investigated the magneto-optical response of Fe and CrO<sub>2</sub> epitaxial films by pump-probe polarimetry, showing that charge and spin dynamics can be unambiguously disentangled. The time-resolved Kerr ellipticity and rotation in the metallic sample are essentially identical after the initial transient (shorter than a picosecond), but they considerably differ in the oxide film, even tens of picoseconds past the optical excitation. These differences are determined by the combined effects of photoexcited charge carriers and spins on the Kerr signal, but a detailed polarimetric analysis can explicitly unravel these contributions. In addition, the diagonal and off-diagonal terms of the dielectric tensor can be retrieved, providing the complete dynamical characterization of magnetic and optical properties in a ferromagnet, which is of utmost importance to understand spin evolution in magnetically correlated complex oxide materials.

DOI: [10.1103/PhysRevB.87.174437](https://doi.org/10.1103/PhysRevB.87.174437)

PACS number(s): 78.20.Ls, 75.70.-i, 78.47.J-

## I. INTRODUCTION

The time-resolved magneto-optical Kerr effect (TR-MOKE) is a well-established technique to investigate the spin dynamics in ferromagnetic layers. It relies on the intensity and polarization changes of light reflected from a magnetic surface after an optical excitation. Thanks to the pump-probe method, the technique can easily achieve time resolution of a few tens of femtoseconds,<sup>1</sup> making it a unique tool to explore ultrafast spin dynamics.

The magnetic information is extracted from the so-called Kerr angle  $\Theta = \theta + i\epsilon$ , a complex quantity that incorporates the light polarization rotation  $\theta$  and ellipticity  $\epsilon$ , both related to the magnetic state of the sample. A long-lasting controversy is whether optical contributions alter the measurement and to what extent the technique is reliable in deriving the true spin dynamics in ferromagnets. As already pointed out by some authors,<sup>2-4</sup> in the ultrashort time window (a few hundreds of femtoseconds past the optical excitation) the dynamics of rotation and ellipticity can differ due to electronic coherence effects,<sup>5</sup> but on a longer time scale  $\theta$  and  $\epsilon$  show identical dynamics. This experimental fact has been considered as proof of genuineness for the technique. However, the investigations were restricted to thin metallic layers in the perturbative regime. Optically induced modifications of the magnetization often employ intense light pulses that cause a large variation of the MOKE signal, well beyond a mere perturbation.<sup>6-10</sup> Therefore, understanding the reliability of the TR-MOKE technique also in the nonperturbative regime becomes of

crucial importance, especially for oxide systems with magnetic correlation where contributions on different time scales are observed<sup>11</sup> and need to be disentangled. Here, we show that even for a long time window (tens of picoseconds), rotation and ellipticity might considerably differ. A detailed analysis of the TR-MOKE signals on two representative cases of ferromagnetic samples reveals that photoexcited charge carriers are responsible for this discrepancy. However, the reliability of the technique is not affected. In particular, it is shown that genuine magnetic information can still be disentangled from nonmagnetic information, provided that both Kerr rotation and ellipticity are measured.

## II. EXPERIMENTAL DETAILS

We have investigated the optically induced spin dynamics in Fe(001) and CrO<sub>2</sub>(100) epitaxial films. Iron has been extensively studied in the past with time-resolved optical methods,<sup>12-14</sup> revealing an extremely fast (<100 fs) and efficient demagnetization upon laser irradiation, typical of simple ferromagnetic metals. Chromium dioxide is a half-metallic ferromagnet with 100% spin polarization at the Fermi level.<sup>15</sup> Its electronic and optical properties have been thoroughly computed,<sup>16-20</sup> and a double-exchange ferromagnetic ordering has been argued.<sup>21,22</sup> Due to the half-metallic character that inhibits spin flip, a slow magnetization dynamics is expected. Previous time-resolved experiments confirmed that optically induced demagnetization occurs on a 100-ps timescale.<sup>11,23</sup>

In our investigation we used films with a thickness larger than the optical penetration depth in order to avoid artifacts due to light reflection at the film-substrate interface. In particular, the Fe(001) film (100 nm thick) has been evaporated on a MgO(001) single crystal, while the CrO<sub>2</sub>(100) film (300 nm thick) has been grown on a TiO<sub>2</sub>(100) substrate by chemical vapor deposition.<sup>24</sup> CrO<sub>2</sub>(100) has a tetragonal crystallographic structure, and the *c* axis (which is also the easy axis of the magnetization) lies in the film plane. The optical analysis has been performed with an amplified Ti:sapphire laser generating 50-fs pulses centered at 800 nm (1.55 eV) with a repetition rate of 1 kHz. Time resolution has been achieved via the pump-probe technique with the pump beam focused on a spot size of about 200 μm and an average fluence of a few mJ/cm<sup>2</sup>. Transient reflectivity, Kerr ellipticity, and rotation have been measured for *p* and *s* polarizations of the probing beam (see Supplemental Material for details<sup>25</sup>).

### III. RESULTS AND DISCUSSION

We begin illustrating the experimental data, with particular emphasis on the differences between the two systems. Figure 1 reports the optical measurements on CrO<sub>2</sub> and Fe. For the sake of clarity, the data are described in a *comparative* manner: each panel in Fig. 1 reports the same kind of measurement but on different samples (CrO<sub>2</sub> on the left-hand side, Fe on the right-hand side). We have restricted our investigation to a time window of 50 ps, neglecting the fine temporal structure around the zero pump-probe delay, which goes beyond the scope of our investigation. As pointed out in Ref. 3, the interpretation of the experiment in terms of the dielectric tensor is truly meaningful past the temporal overlap between pump and probe pulses or after the characteristic electronic dephasing time (tens of femtoseconds in metals). Figure 1(a) shows the temporal evolution of Kerr rotations,  $\theta_s$  and  $\theta_p$ , and ellipticities,  $\epsilon_s$  and  $\epsilon_p$  (the subscripts *p* and *s* label the polarization state of the incident light), as a function of the pump-probe delay. Figure 1(b) reports the same data as in Fig. 1(a), but normalized to the values at negative delay. The normalization clearly highlights how the dynamics of rotations and ellipticities in CrO<sub>2</sub> differ from each other [Fig. 1(b), left]. On the other hand, in Fe all four curves are essentially identical [Fig. 1(b), right]. Figure 1(c) shows the normalized modulus of the Kerr angles for the two polarization states, i.e.,  $|\Theta_s| = (\theta_s^2 + \epsilon_s^2)^{1/2}$  and  $|\Theta_p| = (\theta_p^2 + \epsilon_p^2)^{1/2}$ . In both samples, the normalized Kerr angle is independent of the light polarization. This intriguing result will be clarified in the following discussion. It is, however, interesting to notice how  $|\Theta_s|$  and  $|\Theta_p|$  closely match in CrO<sub>2</sub> [Fig. 1(c), left], despite the different dynamics of rotation and ellipticity shown in Fig. 1(b) (left). The normalized transient reflectivities,  $R_s$  and  $R_p$ , are reported in Fig. 1(d). Regardless of the similar absorbed pump energies (830 J/cm<sup>3</sup> in CrO<sub>2</sub> and 1050 J/cm<sup>3</sup> in Fe; see Supplemental Material), the relative variation of the reflectivity in CrO<sub>2</sub> is an order of magnitude larger than in Fe. This difference depends crucially on the electronic structure of the material, which determines its optical response. In particular, the amplitude of the effect produced by the pump pulse (at 800 nm wavelength) can significantly vary as a function of the probe wavelength (see, e.g., Ref. 13).

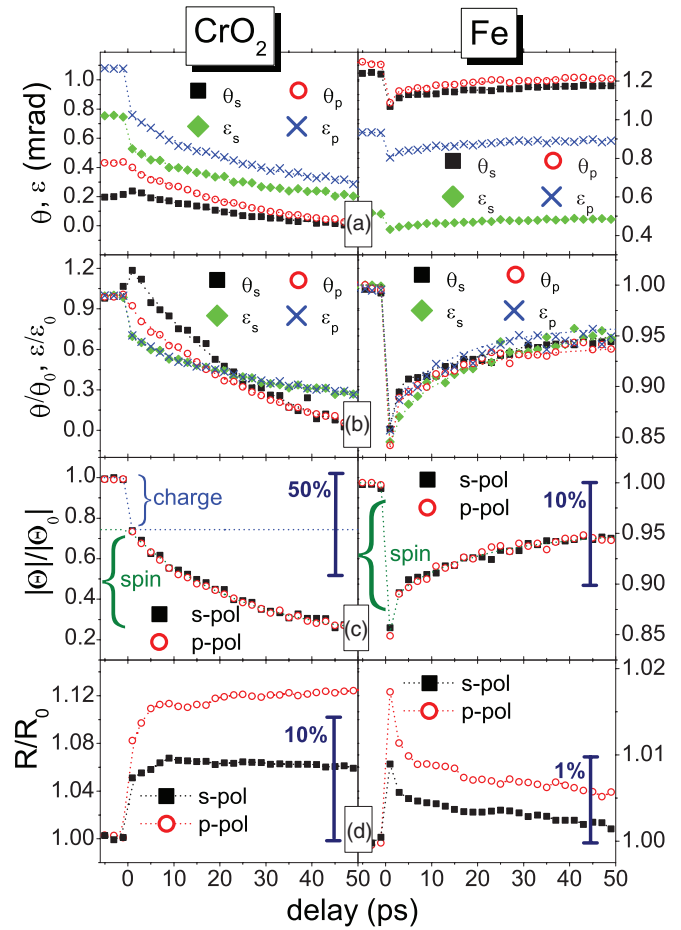


FIG. 1. (Color online) The experimental results for (left) CrO<sub>2</sub> and (right) Fe. (a) Time-resolved Kerr rotations ( $\theta_s$  and  $\theta_p$ ) and ellipticities ( $\epsilon_s$  and  $\epsilon_p$ ). The subscript labels the light polarization state. (b) The same data shown in (a), but normalized to the values at negative delays. (c) Time-resolved normalized Kerr angles  $|\Theta_s| = (\theta_s^2 + \epsilon_s^2)^{1/2}$  and  $|\Theta_p| = (\theta_p^2 + \epsilon_p^2)^{1/2}$ . (d) Normalized transient reflectivities for *p*-polarized and *s*-polarized light. The vertical bars in (c) and (d) help illustrate the amplitude of the effects.

Before proceeding with a more detailed analysis of the data shown in Figs. 1(b) and 1(c), we will clarify why the normalized moduli of the Kerr angles are apparently independent of the light polarization state. According to Jones formalism, *p*- and *s*-polarized light are described by two-dimensional vectors proportional to (1,0) and (0,1), respectively. Reflection from a magnetic surface in the longitudinal MOKE configuration is determined by the following  $2 \times 2$  scattering matrix:<sup>26</sup>

$$\mathbb{M} = \begin{pmatrix} r_{pp} & r_{ps} \\ -r_{ps} & r_{ss} \end{pmatrix}. \quad (1)$$

All matrix elements,  $r_{pp}$ ,  $r_{ss}$ , and  $r_{ps}$ , depend on the light incidence angle (a fixed experimental parameter) and the complex refractive index  $N$ , but only  $r_{ps}$  relates to the sample magnetization via its proportionality to the off-diagonal element of the dielectric tensor  $\epsilon_{xy}$ . The complex Kerr angle is defined as  $\Theta_s = r_{ps}/r_{ss}$  or  $\Theta_p = -r_{ps}/r_{pp}$ , while the reflectivity is  $R_s = |r_{ss}|^2$  or  $R_p = |r_{pp}|^2$ , depending on the polarization state of the incident light. According to these definitions, it is straightforward to show that

$|\Theta_s|/|\Theta_p| = \sqrt{R_p/R_s}$ . The same relation holds for normalized quantities as well. Using the latter, as reported in Figs. 1(c) and 1(d), it can be easily deduced that the ratio  $\sqrt{R_p/R_s}$  never exceeds 1.005 in Fe or 1.03 in CrO<sub>2</sub>. Therefore, the normalized moduli of the Kerr angles measured with *s* or *p* polarization do not differ more than 0.5% in Fe or 3% in CrO<sub>2</sub>.

We can now focus our attention on the magneto-optical data shown in Figs. 1(b) and 1(c). The fact that Kerr rotations and ellipticities of CrO<sub>2</sub> differ from each other raises a fundamental question: which one truly describes the spin dynamics? To provide an appropriate answer we first have to recall that  $\theta$  and  $\epsilon$  (in the following, we drop the *p* and *s* subscripts for clarity) are real and imaginary parts, respectively, of the same complex quantity  $\Theta$ . Therefore, on a first-principles footing,  $\theta$  or  $\epsilon$  alone does not provide an exhaustive magneto-optical knowledge, while only  $\Theta$  contains the complete information. According to the analytical expressions of the matrix elements in Eq. (1) (see Supplemental Material for details), the Kerr angle  $\Theta$  can be written as the product  $f(N) \times \epsilon_{xy}$ , where all the explicit dependence on the refractive index *N* is attributed to the complex function *f*. In particular,  $|\Theta| = |f(N)| \times |\epsilon_{xy}|$ . By invoking linear magneto-optical response, as argued in Ref. 3, we can assert that  $|\epsilon_{xy}| \propto M$ , where *M* is the sample magnetization (a real number). Upon laser irradiation, the temporal variation of  $|\epsilon_{xy}|$  can be affected by charge dynamics as well as spin dynamics, but only the latter modifies *M*. At this point we can reasonably assume that if charge carriers significantly alter  $|\epsilon_{xy}|$ , the effect (both in relative magnitude and the temporal profile) should closely resemble the dynamics of the transient reflectivity, which is only determined by charge evolution.

In the case of Fe, the relative variation of the transient reflectivity [Fig. 1(d), right] is roughly an order of magnitude smaller than the optically induced variation of the Kerr signal [Fig. 1(b), right]. This implies that charge dynamics alters only marginally the functions  $|f(N)|$  and  $|\epsilon_{xy}|$ . Thus, the Kerr signal is dominated by spin dynamics.

The situation is more complex in CrO<sub>2</sub>. The variation of the transient reflectivity is as large as 12% [see Fig. 1(d), left]. Therefore, charge dynamics should give a non-negligible contribution to  $\Theta$ . According to the experimental evidence, the temporal behavior of the reflectivities *R<sub>s</sub>* and *R<sub>p</sub>* displays a prompt change at zero pump-probe delay and a rather flat and featureless dynamics afterwards. On the other hand, all MOKE signals [Figs. 1(b) and 1(c), left] display an exponential-like decay for positive pump-probe delay. This becomes especially evident in Fig. 1(c) (left), i.e., the normalized moduli of the Kerr angle. The prompt variation at zero pump-probe delay resembles the behavior of the transient reflectivity and is therefore attributed to redistribution of hot carriers, as already suggested in previous investigations.<sup>11,23</sup> The subsequent evolution of the signal clearly deviates from the one observed in the reflectivity and is ascribed to the spin dynamics.

In order to quantitatively prove that the prompt variation of the MOKE signal at zero pump-probe delay is due to charge carriers while the subsequent dynamics is determined by spin evolution, we have used the four measured rotations and ellipticities curves of CrO<sub>2</sub> shown in Fig. 1(a) (left) to retrieve the dynamics of the refractive index *N* and the off-diagonal element of the dielectric tensor  $\epsilon_{xy}$ . Rotation and

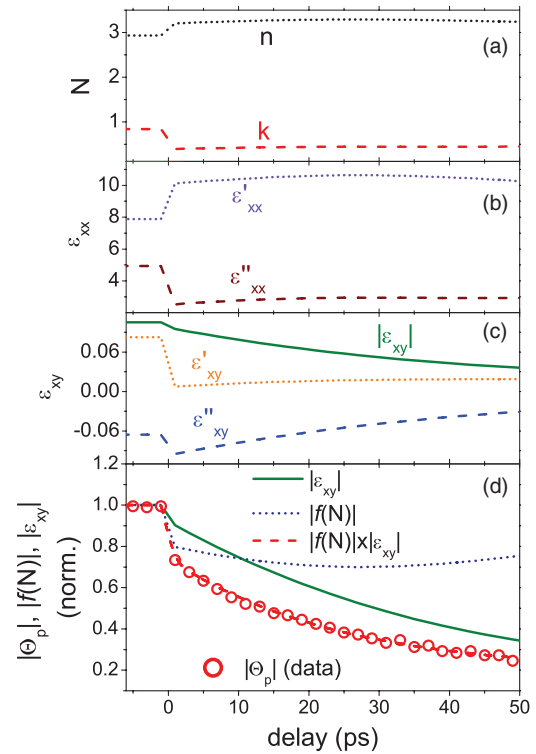


FIG. 2. (Color online) Time evolution of (a) the complex refractive index  $N = n + ik$ , (b) the diagonal term of the dielectric tensor  $\epsilon_{xx} = \epsilon'_{xx} + i\epsilon''_{xx}$ , and (c) the off-diagonal term of the dielectric tensor  $\epsilon_{xy} = \epsilon'_{xy} + i\epsilon''_{xy}$  of CrO<sub>2</sub> as extrapolated from the experimental data shown in Fig. 1(a). (d) Dynamics of the normalized  $|\epsilon_{xy}|$ ,  $|f(N)|$  and  $|f(N)|x|\epsilon_{xy}|$  and a comparison between extracted and measured  $|\Theta_p|$ .

ellipticity can be explicitly written as analytical functions of the complex quantities  $N = n + ik$  and  $\epsilon_{xy} = \epsilon'_{xy} + i\epsilon''_{xy}$  (i.e., four independent variables; see the Supplemental Material). The raw data at positive delay have been fitted with simple exponential decays in order to reduce the uncertainties introduced by data scattering (i.e., experimental error). Using the fits of the experimental measurements  $\theta_s$ ,  $\theta_p$ ,  $\epsilon_s$ ,  $\epsilon_p$  and employing a numerical procedure to invert the analytical functions, we can unambiguously deduce the four quantities  $n$ ,  $k$ ,  $\epsilon'_{xy}$ ,  $\epsilon''_{xy}$ . For completeness, the diagonal term  $\epsilon_{xx}$  of the dielectric tensor can also be obtained from  $n$  and  $k$  using the relation  $\epsilon_{xx} = \epsilon'_{xx} + i\epsilon''_{xx} = (n + ik)^2$ . The results are reported in Figs. 2(a)–2(c). Both  $n$  and  $k$  (as well as  $\epsilon'_{xx}$  and  $\epsilon''_{xx}$ ) show a steep change across the zero pump-probe delay and a rather flat temporal evolution afterward, which is compatible with the observed dynamics of the reflectivity [Fig. 1(d), left]. The dynamical behavior of  $\epsilon'_{xy}$  and  $\epsilon''_{xy}$  (notice their opposite signs) also displays a prompt variation with the pump arrival. However, the modulus  $|\epsilon_{xy}|$  smoothly changes at zero pump-probe delay. If one writes the off-diagonal term in polar form as  $\epsilon_{xy} = |\epsilon_{xy}| \exp(i\phi)$ , it is clear that optical pumping induces a sudden change of the phase  $\phi$ , rather than of the modulus  $|\epsilon_{xy}|$ . An interpretation of this effect would be highly speculative at this stage, and drawing general conclusions on the large class of correlated magnetic oxides (based solely on CrO<sub>2</sub>) would be pretentious, but our finding might provide important information on the electronic and spin

dynamics of optically excited states and should encourage the scientific community to elaborate theoretical corroborations.

According to the above considerations, we can conclude that the modulus  $|\varepsilon_{xy}|$  is not significantly affected by charge carriers. Hence, its dynamics is dominated by the spins (i.e., by  $M$ ). However, the Kerr angle depends also on  $f(N)$  [we recall that  $\Theta = f(N) \times \varepsilon_{xy}$ ]. Using the dynamics of  $n$  and  $k$  reported in Fig. 2(a), we have estimated the evolution of  $|f(N)|$ . The result is shown in Fig. 2(d). As one would expect,  $|f(N)|$  displays a rapid change at zero delay, and it subsequently settles to a constant value. For the sake of clarity, Fig. 2(d) reports also the dynamics of  $|\varepsilon_{xy}|$  and the experimental data  $|\Theta_p|$ . Notice how the extrapolated function  $|f(N)| \times |\varepsilon_{xy}|$  nicely matches the data, providing proof that the prompt variation of the Kerr angle at zero pump-probe delay is determined by charge dynamics [i.e.,  $|f(N)|$ ], while the subsequent evolution genuinely represents the magnetization  $M$ .

#### IV. CONCLUSIONS

In conclusion, we have performed a detailed magneto-optical investigation of two ferromagnetic benchmark systems (Fe and CrO<sub>2</sub>) in order to clarify to what extent the TR-MOKE technique can reliably reveal the spin dynamics. Our analysis shows that a quick comparison between the temporal behavior of the Kerr angle and transient reflectivity is a simple (and recommended) test to judge whether charge dynamics alters the magneto-optical response of the system, which seems to be a special signature of magnetic oxides, or the latter is dominated by the spin evolution, as in the case of Fe. However, this is not a sufficient condition to assert reliability. Exhaustive magneto-optical information is accomplished by measuring both real and imaginary parts of the complex Kerr signal. Restricting the investigation only to rotation or ellipticity might lead to erroneous interpretation of the spin

dynamics, as unveiled by the CrO<sub>2</sub> case. We have shown that the real and imaginary parts of  $\varepsilon_{xy}$ , i.e., the physical quantity carrying the magnetic information, can severely and promptly differ after an optical excitation, although its modulus does not display such features. Even if this effect might bring additional, important information on the electronic configuration of the excited state, it makes the interpretation of magneto-optical response less straightforward. A possible way to overcome this difficulty is to consider the modulus of the Kerr signal (which still requires the measurements of both rotation and ellipticity) since it is unaffected by phase variation of the complex quantities, allowing clearer evidence of a possible optical artifact. Considering the wide usage of the TR-MOKE technique and the ever-increasing number of authors employing this tool to investigate spin dynamics, we believe it is of crucial importance to keep in mind its limitations and subtle criticalities, especially in magnetically correlated complex oxides. Unusual magneto-optical behavior, such as steep change of the signal at zero pump-probe delay and subsequent flat dynamics<sup>27–30</sup> or even prompt enhancement,<sup>31,32</sup> have been recently observed in several magnetic systems and interpreted in terms of genuine spin dynamics. Without any intention to debate the validity of these conclusions, which might be perfectly sound, we point out that a more critical and complete analysis through a detailed experimental effort can undoubtedly verify the magnetic nature of these effects, leading to a considerable benefit for a large scientific community.

#### ACKNOWLEDGMENTS

We thank P. M. Oppeneer for the fruitful and enlightening discussions. We are indebted to A. Calloni for providing us with the Fe(100) film. Fondazione Cariplo is gratefully acknowledged for financial support.

\*ettore.carpene@polimi.it

<sup>1</sup>E. Beaurepaire, J.-C. Merle, A. Daunois, and J.-Y. Bigot, *Phys. Rev. Lett.* **76**, 4250 (1996).

<sup>2</sup>B. Koopmans, M. van Kampen, J. T. Kohlhepp, and W. J. M. de Jonge, *Phys. Rev. Lett.* **85**, 844 (2000).

<sup>3</sup>L. Guidoni, E. Beaurepaire, and J.-Y. Bigot, *Phys. Rev. Lett.* **89**, 017401 (2002).

<sup>4</sup>P. M. Oppeneer and A. Liebsch, *J. Phys. Condens. Matter* **16**, 5519 (2004).

<sup>5</sup>G. P. Zhang, W. Hüubner, G. Lefkidis, Y. Bai, and T. F. George, *Nat. Phys.* **5**, 499 (2009); K. Carva, M. Battiato, and P. M. Oppeneer, *ibid.* **7**, 665 (2011); G. P. Zhang, W. Hüubner, G. Lefkidis, Y. Bai, and T. F. George, *ibid.* **7**, 665 (2011).

<sup>6</sup>K. Vahaplar, A. M. Kalashnikova, A. V. Kimel, D. Hinzke, U. Nowak, R. Chantrell, A. Tsukamoto, A. Itoh, A. Kirilyuk, and Th. Rasing, *Phys. Rev. Lett.* **103**, 117201 (2009).

<sup>7</sup>E. Carpene, C. Piovera, C. Dallera, E. Mancini, and E. Puppini, *Phys. Rev. B* **84**, 134425 (2011).

<sup>8</sup>R. Medapalli, I. Razzdolski, M. Savoini, A. R. Khorsand, A. Kirilyuk, A. V. Kimel, Th. Rasing, A. M. Kalashnikova, A. Tsukamoto, and A. Itoh, *Phys. Rev. B* **86**, 054442 (2012).

<sup>9</sup>J.-Y. Bigot, M. Vomir, L. H. F. Andrade, and E. Beaurepaire, *Chem. Phys.* **318**, 137 (2005).

<sup>10</sup>U. Atxitia, O. Chubykalo-Fesenko, J. Walowski, A. Mann, and M. Münzenberg, *Phys. Rev. B* **81**, 174401 (2010).

<sup>11</sup>G. Müller, J. Walowski, M. Djordjevic, G.-X. Miao, A. Gupta, A. V. Ramos, K. Gehrke, V. Moshnyaga, K. Samwer, J. Schmalhorst, A. Thomas, A. Hütten, G. Reiss, J. S. Moodera, and M. Münzenberg, *Nat. Mater.* **8**, 56 (2009).

<sup>12</sup>T. Kampfrath, R. G. Ulbrich, F. Leuenberger, M. Münzenberg, B. Sass, and W. Felsch, *Phys. Rev. B* **65**, 104429 (2002).

<sup>13</sup>E. Carpene, E. Mancini, C. Dallera, M. Brenna, E. Puppini, and S. De Silvestri, *Phys. Rev. B* **78**, 174422 (2008).

<sup>14</sup>E. Carpene, E. Mancini, C. Dallera, E. Puppini, and S. De Silvestri, *J. Appl. Phys.* **108**, 063919 (2010).

<sup>15</sup>J. M. D. Coey and M. Venkatesan, *J. Appl. Phys.* **91**, 8345 (2002).

<sup>16</sup>S. P. Lewis, P. B. Allen, and T. Sasaki, *Phys. Rev. B* **55**, 10253 (1997).

<sup>17</sup>I. I. Mazin, D. J. Singh, and C. Ambrosch-Draxl, *Phys. Rev. B* **59**, 411 (1999).

<sup>18</sup>N. E. Brener, J. M. Tyler, J. Callaway, D. Bagayoko, and G. L. Zhao, *Phys. Rev. B* **61**, 16582 (2000).

- <sup>19</sup>J. Kuneš, P. Novák, P. M. Oppeneer, C. König, M. Fraune, U. Rüdiger, G. Güntherodt, and C. Ambrosch-Draxl, *Phys. Rev. B* **65**, 165105 (2002).
- <sup>20</sup>H. Brändle, D. Weller, J. C. Scott, J. Sticht, P. M. Oppeneer, and G. Güntherodt, *Int. J. Mod. Phys. B* **7**, 345 (1993).
- <sup>21</sup>M. A. Korotin, V. I. Anisimov, D. I. Khomskii, and G. A. Sawatzky, *Phys. Rev. Lett.* **80**, 4305 (1998).
- <sup>22</sup>P. Schlottmann, *Phys. Rev. B* **67**, 174419 (2003).
- <sup>23</sup>Q. Zhang, A. V. Nurmikko, G. X. Miao, G. Xiao, and A. Gupta, *Phys. Rev. B* **74**, 064414 (2006).
- <sup>24</sup>G. Miao, G. Xiao, and A. Gupta, *Phys. Rev. B* **71**, 094418 (2005).
- <sup>25</sup>See Supplemental Material at <http://link.aps.org/supplemental/10.1103/PhysRevB.87.174437> for detailed description of the experimental setup and the analytical formulation of the ellipsometry quantities.
- <sup>26</sup>Z. J. Yang and M. R. Scheinfein, *J. Appl. Phys.* **74**, 6810 (1993).
- <sup>27</sup>K. Miyasaka, M. Nakamura, Y. Ogimoto, H. Tamaru, and K. Miyano, *Phys. Rev. B* **74**, 012401 (2006).
- <sup>28</sup>D. Steil, S. Alebrand, T. Roth, M. Krauss, T. Kubota, M. Oogane, Y. Ando, H. C. Schneider, M. Aeschlimann, and M. Cinchetti, *Phys. Rev. Lett.* **105**, 217202 (2010).
- <sup>29</sup>S. A. McGill, R. I. Miller, O. N. Torrens, A. Mamchik, I.-W. Chen, and J. M. Kikkawa, *Phys. Rev. Lett.* **93**, 047402 (2004).
- <sup>30</sup>T. Ogasawara, M. Matsubara, Y. Tomioka, M. Kuwata-Gonokami, H. Okamoto, and Y. Tokura, *Phys. Rev. B* **68**, 180407(R) (2003).
- <sup>31</sup>H. Yada, M. Matsubara, H. Yamada, A. Sawa, H. Matsuzaki, and H. Okamoto, *Phys. Rev. B* **83**, 165408 (2011).
- <sup>32</sup>M. Matsubara, Y. Okimoto, T. Ogasawara, Y. Tomioka, H. Okamoto, and Y. Tokura, *Phys. Rev. Lett.* **99**, 207401 (2007).